

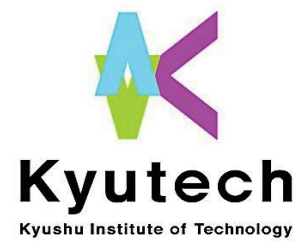


UNIVERSITI PUTRA MALAYSIA

***COMPUTATIONAL FLUID DYNAMICS STUDY OF AIRFLOW AND
PARTICLE DEPOSITION IN DISEASED NASAL AIRWAY***

VIZY NAZIRA BINTI RIAZUDDIN

FK 2018 80



**COMPUTATIONAL FLUID DYNAMICS STUDY OF AIRFLOW AND
PARTICLE DEPOSITION IN DISEASED NASAL AIRWAY**

By

VIZY NAZIRA BINTI RIAZUDDIN

**Thesis Submitted to the School of Graduate Studies, Universiti Putra Malaysia
and Kyushu Institute of Technology, in Fulfilment of the Requirements for the
Degree of Doctor of Philosophy**

February 2018

All material contained within the thesis, including without limitation text, logos, icons, photographs and all other artwork, is copyright material of Universiti Putra Malaysia and Kyushu Institute of Technology unless otherwise stated. Use may be made of any material contained within the thesis for non-commercial purposes from the copyright holder. Commercial use of material may only be made with the express, prior, written permission of Universiti Putra Malaysia and Kyushu Institute of Technology.

Copyright © Universiti Putra Malaysia and Kyushu Institute of Technology.



ACKNOWLEDGEMENT

Alhamdulillah, all praise to Allah for blessing me with opportunity, strength and patience to conduct this study and complete this thesis.

First and foremost, I would like to take this opportunity to thank my supervisors, Assoc. Prof. Ir. Dr. Kamarul Arifin Ahmad and Prof. Dr. Masaaki Tamagawa for their continuous supervision, patient guidance and enthusiastic support throughout my study.

I would also like to express my appreciation to Assoc. Prof. Dr. Mohammad Zubair for his guidance in carrying out this work. My sincere appreciation also goes to Dr. Nur Hashima Abdul Rashid who provided me the CT of upper airway image data so that I could start my research at the first place. I am also very grateful for her thoughtful advices and continuous guidance. I would also like to thank Dr. Norkhairunnisa Mazlan for her helpful advice. I am also grateful to Prof. Dr. Hiroshi Yamada and Prof. Dr. Hiroshi Ishiguro for their research advice. Special thanks also go to Mr. Mohamad Nasir Johari and Mr. Saffairus Salih for their help in setting up my experimental test rig.

I particularly acknowledge the research grant support provided through the Geran Putra Institut Pengajian Siswazah (IPS), project code GP-IPS/2015/9461700 by Universiti Putra Malaysia in carrying out this research work and also the support from Universiti Putra Malaysia through Special Graduate Research Assistant (SGRA) scholarship scheme during the last term of my study. I would also like to thank Japan Student Service Organization (JASSO) for the scholarship provided during my research stay in Japan. I sincerely thank the Malaysian government for the given scholarship through MYBRAIN scheme.

I would also like to thank my research colleague at Kyushu Institute of Technology and Universiti Putra Malaysia for their friendship and joyful memories. I would like to thank my parents, Riazuddin Ahmad Ali and Norizan Osman, and my father and

mother in law, Mohd Suan Tulis and Karsiah Bakri for their endless pray for my success. My sincere gratitude also goes to my dearest husband Mohd Shahadan Mohd Suan for his unconditional love, patience and encouragement through the ups and downs of my PhD journey. Last but not least to my dearest son, Muhammad Eusoff Muzaffar bin Mohd Shahadan, this thesis is dedicated to you.



TABLE OF CONTENTS

CONTENTS		Page
Acknowledgement		i-ii
Table of Contents		iii-vii
List of Figures		viii-xiv
List of Tables		xv
List of Abbreviations		xvi-xvii
List of Publications		xviii-xx
Abstract		xxi-xxiii
 CHAPTER 1: INTRODUCTION		1
1.1	Research Background	1
1.2	Problem Statement	4
1.3	Research Objectives	5
1.4	Scope of Work	6
1.5	Organization of the Thesis	7
 CHAPTER 2: LITERATURE REVIEW		9
2.1	Overview	9
2.2	Anatomy and Physiology of the Human Upper Airway	9
	2.2.1 Upper Airway Anatomy	9
	2.2.2 Upper Airway Physiology	11
2.3	Objective Measurement Methods	12
	2.3.1 Rhinomanometry	12
	2.3.2 Acoustic Rhinometry (AR)	13
	2.3.3 Endoscopy	14
	2.3.4 Polysomnography	14
2.4	Fluid Flow Studies in the Human Upper Airway	15

2.4.1	Computational Model of the Human Nasal Cavity	15
2.4.2	Fluid Flow Modelling	18
2.4.2.1	Velocity and Flow Distribution	18
2.4.2.2	Airflow Resistance	20
2.4.2.3	Wall Shear Stress	20
2.5	Particle Deposition Studies in the Human Nasal Cavity	21
2.5.1	Particle Modelling	22
2.5.2	Factors Affecting Particle Deposition In Nasal Cavity	25
2.5.2.1	Morphology of Respiratory Tract	26
2.5.2.2	Particle Characteristics	26
2.5.2.3	Breathing Flow Rates and Pattern	26
2.6	Upper Airway Surgery	27
2.6.1	Diseased Nasal Airway	27
2.6.2	Obstructive Sleep Apnea (OSA)	31
CHAPTER 3: MODELLING THE HUMAN UPPER AIRWAY		36
3.1	Overview	36
3.2	Developing Three-dimensional Computational Model of the Human Upper Airway	36
3.2.1	Procuring CT Scan Data of Human Upper Airway	38
3.2.2	Converting 2D CT Scans Image to 3D CAD Data	43
3.2.3	Geometry Creation Using CATIA	48
3.3	Hybrid Mesh Generation using ANSYS Workbench	56
3.4	Calculation of First Grid Off the Wall, the y Values	64
3.4.1	Pre-Operative Nasal Computational Model	66
3.4.2	Post-Operative Nasal Computational Model	69

CHAPTER 4: NUMERICAL SIMULATION METHODOLOGY	72
4.1 Overview	72
4.2 Governing Equations for Fluid Phase	72
4.2.1 General Governing Equation for Fluid Flow	72
4.2.2 Reynolds Averaged Navier-Stokes Equations	74
4.3 Governing Equation for Particle Phase	83
4.4 Numerical Solver Procedure	87
4.5 Boundary Condition Definition	93
4.6 Convergence Criteria	97
CHAPTER 5: NUMERICAL INVESTIGATION ON AIRFLOW CHARACTERISTICS IN NASAL CAVITY HAVING TURBINATE HYPERTROPHY, CONCHA BULLOSA, AND SEPTUM DEVIATION WITH OSA: PRE- AND POST SURGERY	98
5.1 Introduction	98
5.2 Methodology	101
5.2.1 Three-Dimensional Nasal Computational Model	101
5.2.2 Numerical Methods	104
5.3 Results and Discussion	105
5.3.1 Grid Dependency Analysis	105
5.3.2 Geometry Comparison	109
5.3.3 Airflow Resistance	115
5.3.4 Velocity and Flow Distribution	117
5.3.5 Pressure Distribution	119
5.3.6 Wall Shear Stress	120
5.3.7 Particle Deposition	123
5.5 Conclusions	125

**CHAPTER 6: COMPUTATIONAL FLUID DYNAMICS STUDY
OF AIRFLOW AND MICROPARTICLE DEPOSITION IN A
CONSTRICTED PHARYNGEAL SECTION REPRESENTING
OBSTRUCTIVE SLEEP APNEA DISEASE**

		126
6.1	Introduction	126
6.2	3D Computational Model Development and Mesh Generation	131
6.3	Numerical Methods	133
6.4	Results And Discussion	134
	6.4.1 Velocity Distribution	134
	6.4.2 Pressure Distribution	139
	6.4.3 Microparticles Deposition	141
6.5	Conclusions	146

**CHAPTER 7: NUMERICAL SIMULATION OF AIRFLOW AND
AEROSOL DEPOSITION IN REALISTIC HUMAN UPPER
AIRWAY WITH OBSTRUCTIVE SLEEP APNEA AND
CHRONIC NASAL OBSTRUCTION: PRE- AND POST-
SURGERY**

		148
7.1	Introduction	148
7.2	Three-Dimensional Upper Airway Computational Model	150
7.3	Numerical Methods	153
7.4	Grid Dependency Analysis	156
7.5	Geometry Creation	158
7.6	Pressure and Flow Resistance	165
7.7	Velocity and Flow Distribution	172
7.8	Wall Shear Stress	178
7.9	Particle Deposition	180
7.10	Conclusions	186

CHAPTER 8: EXPERIMENTAL INVESTIGATION	187
8.1 Introduction	187
8.2 Development of 3D Model	187
8.3 Model Fabrication	190
8.4 Experimental Setup	197
8.5 Experimental Error Analysis	199
8.6 Experimental Results	200
8.7 Comparison of Experimental and Numerical Investigations	203
8.8 Conclusions	205
CHAPTER 9: CONCLUSIONS AND FUTURE RECOMMENDATIONS	206
9.1 Introduction	206
9.2 Conclusions	207
9.3 Future Recommendations	208
REFERENCES	210
APPENDIX I	219
APPENDIX II	220

LIST OF FIGURES

FIGURES		PAGE
Figure 3.1	Flow chart for the present study.	37
Figure 3.2	Coronal CT scan images along the axial distance of the human nasal cavity.	38
Figure 3.3	Coronal CT scan images along the axial distance of the diseased human nasal cavity before surgery.	40
Figure 3.4	Coronal CT scan images along the axial distance of the diseased human nasal cavity after surgery.	41
Figure 3.5	Sagittal plane of CT scan images of human upper airway obtained (a) before surgery and (b) after surgery.	42
Figure 3.6	CT scan images obtained from axial, coronal and sagittal plane and 3D model of the female human nasal cavity.	44
Figure 3.7	CT scan images obtained from axial, coronal and sagittal plane, (a) pre-operative OSA and (b) post-operative OSA.	45
Figure 3.8	Polyline data of the 3D human nasal cavity.	47
Figure 3.9	The 3D model of the diseased human upper airway in .stl file format: (a) pre-operative and (b) post-operative.	48
Figure 3.10	Steps involved in developing 3D model of the nasal cavity using CATIA.	50
Figure 3.11	Modification of control subject to represent OSA disease; (a) normal nasal cavity, (b) upper airway with constricted pharyngeal representing OSA.	51
Figure 3.12	Steps involved in developing 3D model of the diseased human upper airway for the pre-operative case.	53
Figure 3.13	Steps involved in developing 3D model of the diseased human upper airway for post-operative case.	54
Figure 3.14	The three-dimensional pre-operative upper airway model: (a) nasal cavity (b) pharynx.	55
Figure 3.15	The three-dimensional post-operative upper airway model: (a) nasal cavity (b) pharynx.	56
Figure 3.16	Volume mesh of the 3D computational model of human nasal cavity.	57

Figure 3.17	Hybrid mesh generated for the constricted pharyngeal representing OSA model.	58
Figure 3.18	Unstructured tetrahedral mesh generation for the pre-operative nasal cavity model; (a) nasal model in IGES file format (b) volume mesh.	59
Figure 3.19	Unstructured tetrahedral mesh generation for the post-operative nasal cavity model; (a) nasal model in IGES file format (b) volume mesh.	60
Figure 3.20	Tetrahedral mesh generation for pre-operative upper airway model: (a) upper airway model in IGES file format (b) volume mesh.	62
Figure 3.21	Tetrahedral mesh generation for post-operative upper airway model(a) upper airway model in IGES file format (b) volume mesh.	63
Figure 3.22	The measured perimeter at the pharynx section for pre-operative case.	67
Figure 3.23	The measured perimeter at the pharynx section for post-operative case.	70
Figure 4.1	Drag coefficient for spheres as a function of Re_p .	86
Figure 4.2	Control volume used to illustrate discretization of a scalar transport equation.	88
Figure 4.3	Pressure-based solution method.	91
Figure 4.4	Uncoupled discrete phase calculation method.	92
Figure 4.5	Escape boundary condition for the discrete phase.	94
Figure 4.6	Illustration of the particle deposition with trap boundary condition.	95
Figure 5.1	CT scan images for the obstructed nasal airway before surgery.	102
Figure 5.2	CT scan images for the treated nasal airway after surgery.	102
Figure 5.3	Diseased nasal computational model for pre-operative case.	103
Figure 5.4	Diseased nasal computational model for post-operative case.	104

Figure 5.5	Grid dependency study for pre-operative nasal cavity model.	107
Figure 5.6	Grid dependency study for post-operative case nasal cavity model.	108
Figure 5.7	Fourteen cross section area along the axial distance of the nasal cavity for the pre-operative computational model.	110
Figure 5.8	The fourteen planes created for pre-operative nasal cavity.	111
Figure 5.9	Fourteen cross section area along the axial distance of the nasal cavity for the post-operative model.	112
Figure 5.10	The fourteen planes created for post-operative nasal cavity.	113
Figure 5.11	The comparison of cross-sectional area vs. axial distance from anterior to the posterior of the diseased nasal cavity.	114
Figure 5.12	Airflow resistance for flow rates of 7.5 L/min – 40 L/min.	116
Figure 5.13	Pressure drop for inhalation flow rates of 7.5-40 L/min.	117
Figure 5.14	Pathlines for breathing rate of 7.5 L/min for (a) pre-operative and (a) post-operative surgery.	118
Figure 5.15	Comparison of pressure distribution through the nasal airway for pre-operative and post-operative study.	119
Figure 5.16	Comparison of average wall shear stress along the axial distance of the nasal cavity for flow rate of 7.5 L/min.	121
Figure 5.17	Comparison of average wall shear stress for inhalation rate of 20 L/min (a) pre-operative and (b) post-operative.	122
Figure 5.18	Comparison of total deposition efficiency, before and after surgery.	124
Figure 6.1	Left panel shows position of tongue, soft palate, and posterior pharynx during unobstructed breathing in sleeping patients. Right panel shows the position of these structures in OSA patients.	127
Figure 6.2	Computational domain: (a) normal nasal cavity, (b) upper airway with constricted pharyngeal representing Obstructive Sleep Apnea.	132
Figure 6.3	Velocity streamlines for inhalation rates of 7.5 and 20 L/min.	135

Figure 6.4	Velocity vector for inhalation rate of 20 L/min.	137
Figure 6.5	Velocity contour of 20L/min flow rate.	138
Figure 6.6	Recirculation regions downstream of the constricted pharyngeal section.	139
Figure 6.7	Pressure distribution for 20L/min.	140
Figure 6.8	Average static pressure for inhalation rates of 4 to 40 L/min.	141
Figure 6.9	Total deposition efficiency for inhalation rates of 4-40 L/min.	142
Figure 6.10	The six different regions created in the constricted pharyngeal airway model.	143
Figure 6.11	Deposition fraction of microparticles in upper airway for inhalation rates of 7.5 L/min.	144
Figure 6.12	Deposition fraction of microparticles in upper airway for inhalation rates of 20 L/min.	144
Figure 6.13	Comparison of deposition fraction of microparticles deposited in the upper airway for inhalation rate of 7.5 to 40 L/min: (a) Vestibule region	146
Figure 7.1	Comparison of the CT scan images of human upper airway obtained (a) before surgery and (b) after surgery.	151
Figure 7.2	Hybrid mesh generated for the pre-operative upper airway model.	152
Figure 7.3	Hybrid mesh generated for the post-operative upper airway model.	153
Figure 7.4	3D realistic human upper airway computational model with obstructive sleep apnea diseases for pre-operative case.	155
Figure 7.5	3D realistic human upper airway computational model with obstructive sleep apnea disease for post-operative case.	156
Figure 7.6	Grid dependency analysis for pre-operative human upper airway with Obstructive Sleep Apnea.	157
Figure 7.7	Grid dependency analysis for post-operative human upper airway with Obstructive Sleep Apnea.	158

Figure 7.8	Cross section area along the upper airway for the pre-operative computational model.	159
Figure 7.9	The planes created from nasopharynx to larynx region for pre-operative model.	160
Figure 7.10	Cross section area along the upper airway for the post-operative computational model.	161
Figure 7.11	The planes created from nasopharynx to larynx region for post-operative case.	162
Figure 7.12	Cross-sectional area along the axial distance through the nasal airway.	163
Figure 7.13	Cross-sectional area along the sagittal distance through the pharyngeal section.	164
Figure 7.14	Comparison of pressure contour obtained for inhalation rate of 10 L/min: (a) pre- and (b) post-surgery.	166
Figure 7.15	Pressure comparison between pre- and post-operative model for flow rate of 10 L/min.	167
Figure 7.16	Pressure along the pre-operative upper airway model for various flow rates.	168
Figure 7.17	Pressure along the post-operative upper airway model for various flow rates.	169
Figure 7.18	Comparison of airflow resistance plot for inhalation rates ranging from 4 to 10 L/min.	171
Figure 7.19	Velocity vector for inhalation rate of 10L/min, pre-operative case.	173
Figure 7.20	Velocity vector for inhalation rate of 10 L/min, post-operative case.	174
Figure 7.21	Velocity streamlines for inhalation rate of 10 L/min for pre- and post-operative cases.	175
Figure 7.23	Average velocity along pre-operative upper airway for flow rates of 4-10 L/min.	177
Figure 7.24	Average velocity along post-operative upper airway for flow rates of 4-10 L/min.	177
Figure 7.24	Wall shear stress contour on pre-operative upper airway wall for inhalation rate of 10 L/min.	178

Figure 7.25	Comparison of wall shear stress magnitude obtained for inhalation rate 10 L/min: pre- and post-operative model.	180
Figure 7.26	The developed 3D pre-operative upper airway model divided by region	181
Figure 7.27	The developed 3D post-operative upper airway model divided by region	182
Figure 7.28	Comparison of total deposition efficiency for inhalation rate of 4-10 L/min for pre- and post-operative model.	183
Figure 7.29	Particle deposition fraction for inhalation rate of 10 L/min for pre-operation model.	184
Figure 7.30	Particle deposition fraction for inhalation rate of 10 L/min for the post-operative model.	185
Figure 8.1	Pharynx experimental model for the pre-operative case: (a) pharynx, (b) pharynx with connector, (c) extruded 2.5 mm thickness, (d) right part, (e) left part.	188
Figure 8.2	Pharynx experimental model for the post-operative case: (a) pharynx, (b) pharynx with connector, (c) extruded 2.5 mm thickness, (d) right part, (e) left part.	189
Figure 8.3	Stereolithography method.	191
Figure 8.4	Material selection, TuskXC2700T.	192
Figure 8.5	Examples of the printed part with (a) basic, and (b) cosmetic transparent surface finishing	194
Figure 8.6	The transparent model produced from the Rapid Prototyping machine: (a) pre-operative and (b) post-operative.	196
Figure 8.7	Flow measurement apparatus.	197
Figure 8.8	The location of the pressure taps on the pharynx experimental models.	198
Figure 8.9	Pressure drop for pre-operative pharynx model.	201
Figure 8.10	Pressure drop graph for post-operative pharynx model.	201
Figure 8.11	Comparative study of pressure drop plot for numerical and experimental investigation for pre-operative model.	204

Figure 8.12 Comparative study of pressure drop plot for numerical and experimental investigation for post-operative model.



LIST OF TABLES

TABLES	PAGE
Table 2.1 Summary of the specification MRI/CT scans data obtained to develop the nasal computational models.	17
Table 2.2 Summary of grid size, flow rate and viscous models, particle size and particle tracking approach.	25
Table 2.3 Summary of impact of surgical treatment on airflow and aerosol particle deposition.	30
Table 3.1 First grid point off the wall, y value for pre-operative OSA.	68
Table 3.2 First grid point off the wall, y value for post-operative OSA.	71
Table 4.1 The Navier-Stokes equations for incompressible flow	74
Table 4.2 Constants for different intervals of the Reynolds number for the Morsi & Alexander, (2006) drag model.	86
Table 4.3 Summary of the boundary conditions.	93
Table 4.4 Summary of the particle injection properties.	96
Table 4.5 Assumptions for the particle modelling.	97
Table 5.1 Pressure drop for flow rate of 7.5 L/min before and after surgery.	115
Table 7.1 Pressure drop for flow rate of 7.5 L/min before and after surgery.	170
Table 8.1 TuskXC2700T material properties datasheet.	193
Table 8.2 Finishing degrees for Stereolithography parts.	193
Table 8.3 Experimental error measurement for different pressure drop values.	202

LIST OF ABBREVIATIONS

2D	Two Dimensional
3D	Three Dimensional
AR	Acoustic Rhinometry
AAR	Active Anterior Rhinometry
BMI	Body Mass Index
CAD	Computer Aided Design
CFD	Computational Fluid Dynamics
CPAP	Continuous Positive Airway Pressure
CT	Computed Tomography
DE	Deposition Efficiency
DF	Deposition Fraction
DICOM	Digital Imaging and Communications in Medicine
DPM	Discrete Phase Modeling
DSE	Digitized Shape Editor
ENT	Ear Nose and Throat
EPA	Environmental Protection Agency
FESS	Functional Endoscopic Sinus Surgery
FSI	Fluid Structure Interaction
HU	Hounsfield Units
IGES	Initial Graphics Exchange Specification
LES	Large Eddy Simulation
LRN	Low Reynolds Number

MAS	Mandibular Advancement Splint
MMA	Middle Meatal Anstrostomy
MRI	Magnetic Resonance Image
NA	Not Available
NAR	Nasal Airway Resistance
OSA	Obstructive Sleep Apnea
PIV	Particle Image Velocimetry
RANS	Reynolds Averaged Navier Stokes
SST	Shear Stress Transport
UPPP	Uvulopalatopharyngoplasty
US	United States
USM	Universiti Sains Malaysia

LIST OF PUBLICATIONS

Journals

1. **V.N. Riazuddin**, M. Zubair, M. Ahmadi, M. Tamagawa, N.H.A. Rashid, N. Mazlan, K. A. Ahmad, 2016, Computational Fluid Dynamics study of airflow and microparticle deposition in a constricted pharyngeal section representing obstructive sleep apnea disease, *Journal of Medical Imaging and Health Informatics*, 6(6), pp. 1507-1512. (Published)
2. **V.N. Riazuddin**, K. A. Ahmad, M. Tamagawa, M. Zubair, N.H.A. Rashid, N. Mazlan, F. Mustapha, Numerical simulation of airflow and aerosol deposition in realistic human upper airway with chronic nasal obstruction and obstructive sleep apnea: pre- and post-surgery, *PLoS ONE*. (Submitted)
3. M. Ahmadi, M. Zubair, K.A. Ahmad, **V.N. Riazuddin**, Study on nasal deposition of micro particles and its relationship to airflow structure, 2016, *International Journal of Fluids and Heat Transfer*, 1(1), pp. 2-12. (Published)
4. E. Basri, A. Basri, **V.N. Riazuddin**, S.F. Shahwir, M.Zubair, K.A. Ahmad, Computational fluid dynamics study in biomedical applications: A review, 2016, *International Journal of Fluids and Heat Transfer*, 1(2), pp. 2-14. (Published)
5. M. Zubair, **V.N. Riazuddin**, K.A. Ahmad, Numerical study on the effect of gender on the airflow characteristics inside the nasal cavity, 2015, *International Journal of Advanced Thermofluid Research*, 1(1), pp. 2-16. (Published)
6. M. Zubair, **V.N. Riazuddin**, M.Z. Abdullah, I. Rushdan, I.L. Shuaib, K.A. Ahmad, Computational fluid dynamics study of pull and plug flow boundary condition on nasal airflow, 2013, *Biomedical Engineering: Applications, Basis and Communications*, 25(4), pp. 1-8. (Published)
7. M. Zubair, **V.N. Riazuddin**, K.A. Ahmad, S.M.A. Khader, A.A. Basri, Numerical study of a nasal cavity model having a constricted pharyngeal section representing obstructive sleep apnea, 2017, *Journal of Computational Methods in Sciences and Engineering*, 17, pp. 219-226. (Published)

8. M. Zubair, **V.N. Riazuddin**, M.Z. Abdullah, I. Rushdan, I.L. Shuaib, K.A. Ahmad, 2013, Computational fluid dynamics study of the effect of posture on airflow characteristics inside the nasal cavity, *Asian Biomedicine*, 7(6), pp. 835-840.

Conference Presentations

1. **V.N. Riazuddin**, K. A. Ahmad, M. Tamagawa, M. Zubair, M. Ahmadi, N.H.A. Rashid, N. Mazlan, F. Mustapha, Numerical investigation of inspiratory and expiratory airflow in a human upper airway with chronic nasal obstruction and obstructive sleep apnea, 4rd International Conference on Computational Methods in Engineering and Health Sciences (ICCMEH 2017), Manipal University, Kartanaka, India. (19-20 December 2017). (Abstract accepted)
2. **V.N. Riazuddin**, K. A. Ahmad, M. Zubair, M. Tamagawa, N.H.A. Rashid, N. Mazlan, Numerical simulation of airflow in diseased human nasal airway, Mechanical Engineering Research Day 2017 (MERD 2017), Universiti Teknikal Malaysia Melaka, Malaysia (30 March 2017).
3. **V.N. Riazuddin**, K. A. Ahmad, M. Zubair, M. Tamagawa, N.H.A. Rashid, N. Mazlan, Numerical investigation of airflow characteristics in a diseased nasal cavity with OSA: Pre- And Post-surgery, 3rd International Conference on Computational Methods in Engineering and Health Sciences (ICCMEH 2016), Kyushu Institute of Technology, Fukuoka, Japan (17-18 December 2016).
4. **V.N. Riazuddin**, K. A. Ahmad, M. Zubair, M. Tamagawa, N.H.A. Rashid, N. Mazlan, Numerical investigation on airflow characteristics in nasal cavity having turbinate hypertrophy, concha bullosa, and septum deviation: Pre- and Post-surgery, 4th International Symposium on Applied Engineering and Sciences (SAES 2016), Kyushu Institute of Technology, Fukuoka, Japan (17-18 December 2016).
5. **V.N. Riazuddin**, M. Zubair, M. Tamagawa, N.H.A. Rashid, K. A. Ahmad, Computational Fluid Dynamics study of airflow and micro-particles deposition in a constricted pharyngeal representing Obstructive Sleep Apnea, 2nd International Conference on Computational Methods in Engineering and Health Sciences (ICCMEH 2015), Universiti Putra Malaysia, Malaysia (19-20 December 2015).
6. **V.N. Riazuddin**, M. Zubair, M. Tamagawa, N.H.A. Rashid, K. A. Ahmad, Computational Fluid Dynamics study of airflow in upper airway with Obstructive

- Sleep Apnea- A Review, Biomedical Fuzzy System Association 2015 (BMFSA 2015), Tokai University, Kumamoto, Japan (21-22 November 2015).
7. M. Ahmadi, M. Kojourimanesh, M. Zubair, **V.N. Riazuddin**, CFD analysis of mucus effect in the nasal cavity, 4rd International Conference on Computational Methods in Engineering and Health Sciences (ICCMEH 2017), Manipal University, Kartanaka, India. (19-20 December 2017).
 8. M. Ahmadi, M. Zubair, **V.N, Riazuddin**, K.A. Ahmad, Study on nasal deposition of micro particles and its relationship to airflow structure, 2nd International Conference on Computational Methods in Engineering and Health Sciences, Universiti Putra Malaysia, Malaysia (19-20 December 2015).
 9. E. Basri, M. Zubair, **V.N Riazuddin**, K.A. Ahmad, Computational fluid dynamics study in biomedical applications, 2nd International Conference on Computational Methods in Engineering and Health Sciences, Universiti Putra Malaysia, Malaysia (19-20 December 2015).
 10. M. Tamagawa, R. Motooka, **V.N. Riazuddin**, K.A. Ahmad, CFD based prediction of Thrombus Formation Rate in Shear Blood Flows, Symposium on Applied Engineering and Sciences, Kyushu Institute of Technology, Japan (20-21 December 2014).

ABSTRACT

COMPUTATIONAL FLUID DYNAMICS STUDY OF AIRFLOW AND PARTICLE DEPOSITION IN DISEASED NASAL AIRWAY

Understanding the properties of airflow in the nasal cavity is very important in determining the nasal physiology and in diagnosis of various anomalies associated with the nose. The complex anatomy of the nasal cavity has proven to be a significant obstacle in the understanding of nasal obstructive disorders. Due to their non-invasiveness, Computational Fluid Dynamics (CFD) has now been utilized to assess the effects of surgical interventions on nasal morphological changes as well as local breathing airflow characteristics through the upper airway of individual patients. Furthermore, nasal inhalation is a major route of entry into body for airborne pollutions. Therefore, the function of the upper airway to filter out the inhaled toxic particles is considered important. The determination of the total particle filtering efficiency and the precise location of the induced lesion in the upper airway is the first step in understanding the critical factors involved in the pathogenesis of the upper airway injury. The present work involved development of three-dimensional diseased upper airway models from Computed Tomographic (CT) scan images derived from a nasal airway without any nasal diseased and an upper airway which was diagnosed with chronic nasal obstruction and obstructive sleep apnea. Numerical simulation of airflow and transport and deposition of inhaled pollutant through chronic diseased nasal airway, constricted pharyngeal representing Obstructive Sleep Apnea (OSA) and diseased upper airway with OSA for pre- and post-operative cases have been studied. Detailed flow pattern and characteristics for inspiratory airflow for various breathing rates (7.5-40 L/min) were evaluated. Simulation of the particle transport and

deposition of micro-sized particles with particle diameter ranging from 1-40 μm were also investigated. In the first part of this study, the surgical treatment performed in the nasal cavity which include septoplasty, inferior turbinate reduction and partial concha bullosa resection substantially increased nasal volume, which influenced flow partitioning and decreases the pressure drop and flow resistance of the nasal passage. The removal of the obstruction in the nasal airway significantly improve the breathing quality. However, the nasal airway experienced approximately about a 50 % decrease in total particle filtering efficiency after surgery. Therefore, careful consideration should be given to this matter before nasal operation especially for a patient with breathing allergic history. In the second part of this study, the morphology of the constricted pharyngeal representing OSA was found to significantly affect the airflow pattern and the deposition fraction of microparticles. The morphology of the upper airway, the size of the inhaled particle and breathing rate was found significantly affect the total particle deposition efficiency and local deposition fraction in the upper airway. The presented regional deposition fraction may be used in specifying the site of highest possibility for respiratory lesions according to the breathing rate and the size of the inhaled toxic particles. Results obtained from this study can be also used to estimate the location of airway obstruction in upper airway of patient with sleep apnea symptom. In the third part of this study, the surgical conducted procedure has cleared out the obstructions in the nasal airway hence improve the airflow distribution through the upper airway during inhalation process. This study shows that the nasal surgery alone can help improve the breathing quality in the upper airway with OSA. The reduction of the airflow resistance in the nasal cavity affect the pressure distribution in the lower part of the upper airway. Obstruction in the nasal passage and sudden airway expansion in the upper airway increased number of particles trap, recirculated and finally

deposited in the airway. Finally, the experimental data obtained from the experimental study utilizing the developed pharyngeal airway further validate the result obtained from the numerical study.





© COPYRIGHT UPM

CHAPTER 1

INTRODUCTION

1.1 Research Background

Upper airway which consisted of nasal cavity and pharynx is one of the most important components of human respiratory system. It provides the first line protection for lung by warming and humidifying the inspired air. Upper airway plays an important role to filter out the inhaled air from airborne contaminated particles, bacteria and pathogen. However, the success of upper airway physiological function is highly dependent on the fluid dynamics characteristic of airflow through the airway passage. Hence, better understanding of airflow characteristic and transport and deposition of inhaled particle through the upper airway is essential to understand the physiology of upper airway breathing pattern.

During inhalation, upper airway also plays an important role to filter out the inhaled toxic and contaminated particles from the polluted atmospheric air. Both the fine and coarse particles which enter the breathing airway during inhalation, not only can induce irritation, moreover, with extensive exposure and high concentration of inhaled airborne toxic and infectious particle, the airway is susceptible to chronic injury and could further aggravate upper airway disorder (Harkema *et al.*, 2006). Harkema *et al.*, (2006) and Grotberg (2001) also reported that the determination of the precise location of the induced lesion in the upper airway is the first step in understanding the critical factors involved in the pathogenesis of the upper airway

injury. As we already know that the toxic and contaminated particles could harm and affect the health of the human population. Hence it is important to investigate and improve understanding of the airflow distribution and particle transport and deposition in the human nasal airway. The location of the particle deposition in an airway is important information for correlating inhaled toxins or carcinogens to disease locations and for developing potential therapies.

Airflow through human upper airway has been studied numerically and experimentally by a number researchers (Garcia *et al.*, 2007; Kim & Chung, 2004; Mylavaram *et al.*, 2009; Segal *et al.*, 2008; Weinhold & Mlynski, 2004; Wen *et al.*, 2008; Xiong *et al.*, 2008). Furthermore, several researchers have undertaken studies pertaining to airflow through nasal cavity using measuring devices such as rhinomanometry and acoustic rhinometry (Hilberg *et al.*, 1989; Jones & Lancer, 1987; Shelton & Eiser, 1992; Sipila & Suonpaa, 1997; Suzina *et al.*, 2003).

Rhinomanometry is used to measure the pressure required to produce airflow through the nasal airway and acoustic rhinometry is used to measure the cross-sectional area of the airway at various nasal planes. However, measuring the precise velocity of airflow and evaluating the local nasal resistance in every portion of the nasal cavity have proven to be difficult (Ishikawa *et al.*, 2009). The anatomical complexity of the nasal cavity makes it difficult for the measurement of nasal resistance. The small sizes of the nasal cavity and its narrow flow passage can cause perturbations in the airflow with any inserted probe. Moreover, the reliability of the result obtained using this device depends on optimal cooperation from the subject, correct instructions from the investigator, and standardized techniques (Kjaergaard *et*

al., 2009). There are reports of failure rates of between 25 % and 50 % in the subjects examined by rhinomanometry (Austin & Foreman, 1994). Furthermore, direct measurement of the total particle deposition efficiency and local deposition fraction of inhaled contaminated particle in the human upper airway are highly impossible.

Due to the inherent limitations of the available measuring devices, Computational Fluid Dynamics (CFD) has been proposed as a viable alternative. CFD which refers to use of numerical methods to solve the partial differential equation governing the flow of a fluid, is becoming an increasingly popular research tool in fluid dynamics (Basri *et al.*, 2016). The non-invasive CFD modelling allows investigation of a wide variety of flow situations and particle deposition through human upper airway. Several researchers have conducted studies on the airflow and particle transport and deposition through the human upper airway by using the CFD simulation technique (Abouali *et al.*, 2012; Bahmanzadeh *et al.*, 2015; Dastan *et al.*, 2014; Ghalati *et al.*, 2012; Riazuddin *et al.*, 2011).

In the present study, initially the effect of nasal obstruction which include septum deviation, turbinate hypertrophy and concha bullosa were investigated. A comparative study was made between the pre- and post-operative model. The effect of nasal surgery on inhaled particle filtering function was also investigated. In order to improve the understanding of the pathophysiology of the Obstructive Sleep Apnea (OSA) disease, numerical simulation of inspiratory airflow through a constricted pharyngeal section representing OSA symptom was conducted. Studies were carried out for various flow rates of 7.5 L/min, 10 L/min, 20 L/min, 30 L/min and 40 L/min suggesting various breathing rates. Lagrangian particle tracking approach was used to

investigate the effect of the constricted pharyngeal section on the deposition rate and deposition patterns of microparticles. Microparticles in the size range of 1-40 μm were injected at the nostril inlet and the particle trajectories and regional deposition fractions of the particles were analyzed.

In order to investigate the effect of chronic nasal obstruction on the upper airway diagnosed with OSA disease, numerical simulation of airflow and aerosol deposition in a realistic human upper airway with chronic nasal airway and obstructive sleep apnea symptom for pre- and post-surgery were performed. Different inhalation rates of steady laminar airflows suggesting low breathing activity were simulated numerically through the upper airway models. The airflow characteristics and breathing resistance were analyzed. Lagrangian trajectory analysis approach was used to examine the transport and deposition of the inhaled microparticles through the upper airways before and after surgery. The focus of the final part of this study is to develop an experimental setup and perform experimental work on a pharyngeal airway model to compare and validate the results obtained from numerical study with that of experiment.

1.2 Problem Statement

Although treatment methods in upper airway surgery have constantly improved over time, due to the narrow and complicated structure of the human nasal airway and anatomical differences between each individual, the prediction of a successful individual therapy remains a challenging task. Hence, further studies are needed to improve the diagnosis method and the quality of the future upper airway surgical treatment. The highly detailed anatomy of the pre- and post-operative morphological

upper airway model and information derived from CFD analysis would be able to provide relevant information prior to a surgical intervention and medical treatment. The analyzed data of detailed aerodynamic behavior of the upper airways can be made available to the ENT surgeons so that it can be used to assist them in identifying possible sites of obstruction and direct toward the anatomic site of obstruction for surgical intervention. The location of the particle deposition in an airway can provide important information for correlating inhaled toxins or carcinogens to disease locations and for developing potential therapies. The main outcome will lead to the improvement of the diagnostics methodologies or even improved treatment strategies and outcome.

1.3 Research Objectives

The overall objective of the present study is focused on the investigation of the airflow characteristics and inhaled particle deposition in the diseased human upper airway. The main aims include:

- i. To develop a three-dimensional computational model of human nasal airway for pre- and post-operative nasal computational models.
- ii. To perform CFD analysis on both the pre- and post-operative diseased nasal airway.
- iii. To analyze the impact of abnormal nasal passage on airflow characteristics and aerosol deposition.
- iv. To investigate the effect of deformation of the pharyngeal section on the airflow and particle deposition in the human upper airway.

- v. To develop experimental setup and perform experimental study to validate the results obtained from the numerical study.

1.4 Scope of Work

This research work was first carried out by procuring Computed Tomography (CT) scan images of the normal and diseased human upper airway. For the normal nasal airway, the CT scan data was provided by a radiologist from the Advanced Medical and Dental Institute, Universiti Sains Malaysia. For the diseased upper airway, the CT scan data was provided by a Head and Neck Surgeon from Hospital Serdang, Malaysia. A research proposal was prepared and submitted to the committee of the Clinical Research Centre and the Medical Research and Ethics Committee, Ministry of Health Malaysia to obtain research approval. The ethical approval letter issued by the committees are as presented in Appendix I and II in this thesis.

A normal nasal cavity of 39-year-old Malaysian female was selected for the normal nasal cavity model whereas a 38-year-old Malaysian male diagnosed with chronic nasal obstruction and prevalence of OSA were selected for this diseased upper airway study. The selected CT scan data were imported into an image processing software, Mimics in order to process the scan images and to generate a realistic three-dimensional computational aided design CAD model of the upper airways. This was then followed by construction of three-dimensional surface geometry by using a Computer Aid Design (CAD) software CATIA.

The 3D surface geometries were imported into GAMBIT, ANSYS ICEM CFD and ANSYS FLUENT Meshing for unstructured and hybrid mesh generation. Numerical simulation of airflow and particle transport and deposition were further carried out by using the available CFD commercial software, ANSYS FLUENT. Numerical inspiratory airflow was simulated for various breathing rates which includes 4, 7.5, 10, 20, 30 and 40 L/min. Particles were injected into the upper airway from the nostril inlet to investigate the transport and deposition in the upper airway. The size of the injected particle includes 1, 5, 10, 20 and 40 μm . Experimental test rig was developed, pharynx experimental model was fabricated, and experimental investigation was conducted to compare and validate the results obtained from the numerical study with that of the experimental results.

1.5 Organization of the Thesis

This thesis includes 9 chapters. The first chapter provides an introduction that review relevant research objectives, and related outlines of the purposes of this study. Chapter 2 presents an in-depth review of the background for the research. The chapter begins with an introduction to the anatomy and physiological function of the human upper airway and is followed by a review of previous studies related to the research. Chapter 3 presents the method used to construct and develop the three-dimensional realistic diseased human upper airway from the CT scan data. Chapter 4 presents the numerical method used to perform CFD simulation of airflow and particle transport and deposition in the upper airway computational model. Chapter 5 presents the numerical investigation on airflow characteristics and particle deposition in diseased nasal cavity having turbinate hypertrophy, concha bullosa, and septum deviation. A comparative study was made between pre- and post-operative model. Chapter 6

presents the computational fluid dynamics study of airflow and micro-particle deposition in a constricted pharyngeal section representing obstructive sleep apnea disease. Chapter 7 presents numerical simulation of airflow and aerosol deposition in realistic human upper airway with obstructive sleep apnea and chronic nasal obstruction for pre- and post-surgery. Chapter 8 presents the method used to develop the pharynx experimental model and the experiment test rig for both pre and post-operative cases. The main aim of this study was to analyze and validate the solutions obtained from numerical study. Finally, Chapter 9 presents the summary of the major research findings derived from the research studied. Suggestions for future works are also presented in this chapter.

REFERENCES

- Abouali, O., Keshavarzian, E., Farhadi Ghalati, P., Faramarzi, A., Ahmadi, G., & Bagheri, M. H. (2012). Micro and nanoparticle deposition in human nasal passage pre and post virtual maxillary sinus endoscopic surgery. *Respiratory Physiology and Neurobiology*, *181*(3), 335–345. <http://doi.org/10.1016/j.resp.2012.03.002>
- ANSYS FLUENT Theory Guide. (2009). Theory Guide Release 12.0. *ANSYS Inc.*
- Austin, C. E., & Foreman, J. C. (1994, January). Acoustic rhinometry compared with posterior rhinomanometry in the measurement of histamine- and bradykinin-induced changes in nasal airway patency. *British Journal of Clinical Pharmacology*.
- Bahmanzadeh, H., Abouali, O., Faramarzi, M., & Ahmadi, G. (2015). Numerical simulation of airflow and micro-particle deposition in human nasal airway pre- and post-virtual sphenoidotomy surgery. *Computers in Biology and Medicine*, *61*, 8–18. <http://doi.org/10.1016/j.compbiomed.2015.03.015>
- Bailie, N., Hanna, B., Watterson, J., & Gallagher, G. (2006). An overview of numerical modelling of nasal airflow. *Rhinology*, *44*(1), 53–57.
- Banabilh, S. M., Suzina, a. H., Mohamad, H., Dinsuhaimi, S., Samsudin, a. R., & Singh, G. D. (2010). Assessment of 3-D nasal airway morphology in Southeast Asian adults with obstructive sleep apnea using acoustic rhinometry. *Clinical Oral Investigations*, *14*(5), 491–498. <http://doi.org/10.1007/s00784-009-0342-9>
- Basri, E. I., Basri, A. A., Riazuddin, V. N., Farhana, S., Zuber, M., & Ahmad, K. A. (2016). Computational Fluid Dynamics Study in Biomedical Applications : A Review. *International Journal of Fluid and Heat Transfer*, *1*(2), 2–14.
- Cheng, Y. S. (2003). Aerosol Deposition in the Extrathoracic Region. *Aerosol Science and Technology*, *37*(8), 659–671. <http://doi.org/10.1080/02786820300906>
- Cho, K., & Cho, Y. (1994). Acute lung disease after exposure to fly ash. *Chest ...*, 309–311. Retrieved from <http://journal.publications.chestnet.org/article.aspx?articleid=1067670>
- Chouly, F., Van Hirtum, a., Lagrée, P. Y., Pelorson, X., & Payan, Y. (2008). Numerical and experimental study of expiratory flow in the case of major upper airway obstructions with fluid-structure interaction. *Journal of Fluids and Structures*, *24*(2), 250–269. <http://doi.org/10.1016/j.jfluidstructs.2007.08.004>
- Chung, S.-K., Son, Y. R., Shin, S. J., & Kim, S.-K. (2006). Nasal airflow during respiratory cycle. *American Journal of Rhinology*, *20*(4), 379–384. <http://doi.org/10.2500/ajr.2006.20.2890>
- Corey, J. P. (2006). Acoustic rhinometry: should we be using it? *Current Opinion in Otolaryngology & Head and Neck Surgery*, *14*(1). Retrieved from http://journals.lww.com/otolaryngology/Fulltext/2006/02000/Acoustic_rhinometry__should_we_be_using_it_.7.aspx
- Croce, C., Fodil, R., Durand, M., Sbirlea-Apiou, G., Caillibotte, G., Papon, J. F., ...

- Louis, B. (2006). In Vitro Experiments and Numerical Simulations of Airflow in Realistic Nasal Airway Geometry. *Annals of Biomedical Engineering*, 34(6), 997–1007. <http://doi.org/10.1007/s10439-006-9094-8>
- Dastan, A., Abouali, O., & Ahmadi, G. (2014). CFD simulation of total and regional fiber deposition in human nasal cavities. *Journal of Aerosol Science*, 69, 132–149. <http://doi.org/10.1016/j.jaerosci.2013.12.008>
- De Backer, J. W., Vanderveken, O. M., Vos, W. G., Devolder, a., Verhulst, S. L., Verbraecken, J. a., ... De Backer, W. a. (2007). Functional imaging using computational fluid dynamics to predict treatment success of mandibular advancement devices in sleep-disordered breathing. *Journal of Biomechanics*, 40(16), 3708–3714. <http://doi.org/10.1016/j.jbiomech.2007.06.022>
- Doorly, D., Taylor, D. J., Franke, P., & Schroter, R. C. (2008). Experimental investigation of nasal airflow. *Proceedings of the Institution of Mechanical Engineers. Part H, Journal of Engineering in Medicine*, 222(4), 439–453. <http://doi.org/10.1007/s10439-005-4388-9>
- Eccles, R. (1998). The relationship between subjective and objective measures of nasal function. *Japan Rhinologic Society*, 37(2), 61–69.
- Elad, D., Liebenthal, R., Wenig, B. ., & Einav, S. (1993). Analysis of airflow patterns in the human nose. *Medical and Biomedical Engineering and Computing*, (November), 585–592.
- Elad, D., Wolf, M., & Keck, T. (2008). Air-conditioning in the human nasal cavity. *Respiratory Physiology & Neurobiology*, 163(1–3), 121–127. <http://doi.org/10.1016/j.resp.2008.05.002>
- Ephros, H. D., Madani, M., & Yalamanchili, S. C. (2010). Surgical treatment of snoring & obstructive sleep apnoea. *The Indian Journal of Medical Research*, 131(February), 267–276.
- Farhadi Ghalati, P., Keshavarzian, E., Abouali, O., Faramarzi, A., Tu, J., & Shakibafard, A. (2012). Numerical analysis of micro- and nano-particle deposition in a realistic human upper airway. *Computers in Biology and Medicine*, 42(1), 39–49. <http://doi.org/10.1016/j.compbiomed.2011.10.005>
- Fogel, R. B., Malhotra, A., & White, D. P. (2004). Sleep · 2: Pathophysiology of obstructive sleep apnoea/hypopnoea syndrome, (February 2008), 159–164. <http://doi.org/10.1136/thx.2003.015859>
- Garcia, G. J. M., Bailie, N., Martins, D. a, & Kimbell, J. S. (2007). Atrophic rhinitis: a CFD study of air conditioning in the nasal cavity. *Journal of Applied Physiology (Bethesda, Md. : 1985)*, 103(3), 1082–1092. <http://doi.org/10.1152/jappphysiol.01118.2006>
- Ghahramani, E., Abouali, O., Emdad, H., & Ahmadi, G. (2014). Numerical analysis of stochastic dispersion of micro-particles in turbulent flows in a realistic model of human nasal/upper airway. *Journal of Aerosol Science*, 67, 188–206. <http://doi.org/10.1016/j.jaerosci.2013.09.004>
- Grotberg, J. B. (2001). and T Ransport P Rocesses. *Transport*.

- Guha, A. (2008). Transport and Deposition of Particles in Turbulent and Laminar Flow. *Annual Review of Fluid Mechanics*, 40(1), 311–341. <http://doi.org/10.1146/annurev.fluid.40.111406.102220>
- Guilleminault, C., Tilkian, a, & Dement, W. C. (1976). The sleep apnea syndromes. *Annual Review of Medicine*, 27, 465–484. <http://doi.org/10.1146/annurev.me.27.020176.002341>
- Hahn, I., Scherer, P. W., & Mozell, M. M. (1993). Velocity profiles measured for airflow through a large-scale model of the human nasal cavity. *J Appl Physiol*, 75(5), 2273–2287. Retrieved from <http://jap.physiology.org/content/75/5/2273>
- Harkema, J. R., Carey, S. a, & Wagner, J. G. (2006). The nose revisited: a brief review of the comparative structure, function, and toxicologic pathology of the nasal epithelium. *Toxicologic Pathology*, 34(3), 252–269. <http://doi.org/10.1080/01926230600713475>
- Heyder, J. (2004). Deposition of inhaled particles in the human respiratory tract and consequences for regional targeting in respiratory drug delivery. *Proceedings of the American Thoracic Society*, 1(4), 315–320. <http://doi.org/10.1513/pats.200409-046TA>
- Heyder, J., Gebhart, J., Rudolf, G., Schiller, C. F., & Stahlhofen, W. (1986). Deposition of particles in the human respiratory tract in the size range 0.005–15 μm .pdf. *Journal of Aerosol Science*, 17(5), 811–825.
- Hilberg, O., Jackson, A. C., Swift, D. L., & Pedersen, O. F. (1989). Acoustic rhinometry: evaluation of nasal cavity geometry by acoustic reflection. *Journal of Applied Physiology (Bethesda, Md. : 1985)*, 66(1), 295–303.
- Hopkins, L. M., Kelly, J. T., Wexler, a. S., & Prasad, a. K. (2000). Particle image velocimetry measurements in complex geometries. *Experiments in Fluids*, 29(1), 91–95. <http://doi.org/10.1007/s003480050430>
- Inthavong, K., Wen, J., Tian, Z., & Tu, J. (2008). Numerical study of fibre deposition in a human nasal cavity. *Journal of Aerosol Science*, 39(3), 253–265. <http://doi.org/10.1016/j.jaerosci.2007.11.007>
- Inthavong, K., Zhang, K., & Tu, J. (2009). Modelling Submicron and Micron Particle Deposition in a Human Nasal Cavity. *Seventh International Conference on CFD Inthe Minerals and Process Industries CSIRO, Melbourne, Australia*, (December), 1–7.
- Ishikawa, S., Nakayama, T., Watanabe, M., & Matsuzawa, T. (2009). Flow Mechanisms in the Human Olfactory Groove. *Archives of Otolaryngology--Head & Neck Surgery*, 135(2), 156–162. <http://doi.org/10.1001/archoto.2008.530>
- Ito, Y., Cheng, G. C., Shih, A. M., Koomullil, R. P., Soni, B. K., Sittitavornwong, S., & Waite, P. D. (2011). Patient-specific geometry modeling and mesh generation for simulating Obstructive Sleep Apnea Syndrome cases by Maxillomandibular Advancement. *Mathematics and Computers in Simulation*, 81(9), 1876–1891. <http://doi.org/10.1016/j.matcom.2011.02.006>
- Jayaraju, S. T. (2009). *Study of the air flow and aerosol transport in the human upper airway using LES and DES Methodologies*. Vrije Universiteit Brussel.

- Jeong, S. J., Kim, W. S., & Sung, S. J. (2007). Numerical investigation on the flow characteristics and aerodynamic force of the upper airway of patient with obstructive sleep apnea using computational fluid dynamics. *Medical Engineering & Physics*, 29(6), 637–651. <http://doi.org/10.1016/j.medengphy.2006.08.017>
- Jones, A. S., & Lancer, J. M. (1987). Rhinomanometry. *Clinical Otolaryngology & Allied Sciences*, 12(3), 233–236. <http://doi.org/10.1111/j.1365-2273.1987.tb00193.x>
- Karakosta, P., Alexopoulos, A. H., & Kiparissides, C. (2013). Computational model of particle deposition in the nasal cavity under steady and dynamic flow. *Computer Methods in Biomechanics and Biomedical Engineering*, 18(5), 514–526. <http://doi.org/10.1080/10255842.2013.819856>
- Keyhani, K., Scherer, P. W., & Mozell, M. M. (1995). Numerical simulation of airflow in the human nasal cavity. *Journal of Biomechanical Engineering*, 117(4), 429–441. <http://doi.org/10.1115/1.2794204>
- Keyhani, K., Scherer, P. W., & Mozell, M. M. (1997). A numerical model of nasal odorant transport for the analysis of human olfaction. *Journal of Theoretical Biology*, 186(3), 279–301. <http://doi.org/10.1006/jtbi.1996.0347>
- Kim, S. K., & Chung, S. K. (2004). An investigation on airflow in disordered nasal cavity and its corrected models by tomographic PIV. *Measurement Science and Technology*, 15(6), 1090–1096. <http://doi.org/10.1088/0957-0233/15/6/007>
- Kim, S. K., Na, Y., Kim, J. I., & Chung, S. K. (2013). Patient specific CFD models of nasal airflow: Overview of methods and challenges. *Journal of Biomechanics*, 46(2), 299–306. <http://doi.org/10.1016/j.jbiomech.2012.11.022>
- Kimbell, J. S., Frank, D. O., Laud, P., Garcia, G. J. M., & Rhee, J. S. (2013). Changes in nasal airflow and heat transfer correlate with symptom improvement after surgery for nasal obstruction. *Journal of Biomechanics*, 46(15), 2634–2643. <http://doi.org/10.1016/j.jbiomech.2013.08.007>
- Kjaergaard, T., Cvancarova, M., & Steinsvag, S. K. (2009). Relation of nasal air flow to nasal cavity dimensions. *Archives of Otolaryngology--Head & Neck Surgery*, 135(6), 565–570. <http://doi.org/10.1001/archoto.2009.50>
- Lal, D., & Corey, J. P. (2004). Acoustic rhinometry and its uses in rhinology and diagnosis of nasal obstruction. *Facial Plastic Surgery Clinics of North America*, 12(4), 397–405, v. <http://doi.org/10.1016/j.fsc.2004.04.002>
- Lindemann, J., Brambs, H. J., Keck, T., Wiesmiller, K. M., Rettinger, G., & Pless, D. (2005). Numerical simulation of intranasal airflow after radical sinus surgery. *American Journal of Otolaryngology - Head and Neck Medicine and Surgery*, 26(3), 175–180. <http://doi.org/10.1016/j.amjoto.2005.02.010>
- Lipton, A. J., & Gozal, D. (2003). Treatment of obstructive sleep apnea in children: do we really know how? *Sleep Medicine Reviews*, 7(1), 61–80. <http://doi.org/10.1053/smr.2001.0256>
- Liu, Y., Matida, E. a., Gu, J., & Johnson, M. R. (2007). Numerical simulation of aerosol deposition in a 3-D human nasal cavity using RANS, RANS/EIM, and

- LES. *Journal of Aerosol Science*, 38(7), 683–700. <http://doi.org/10.1016/j.jaerosci.2007.05.003>
- Lu, M. Z., Liu, Y., Ye, J. Y., & Luo, H. Y. (2014). Large Eddy Simulation of Flow in Realistic Human Upper Airways with Obstructive Sleep. *Procedia Computer Science*, 29, 557–564. <http://doi.org/10.1016/j.procs.2014.05.050>
- Mamikoglu, B., Houser, S., Akbar, I., Ng, B., & Corey, J. P. (2000). Acoustic rhinometry and computed tomography scans for the diagnosis of nasal septal deviation, with clinical correlation. *Otolaryngology--Head and Neck Surgery: Official Journal of American Academy of Otolaryngology-Head and Neck Surgery*, 123(1 Pt 1), 61–68. <http://doi.org/10.1067/mhn.2000.105255>
- Menter, F. R. (1994). Two-equation eddy-viscosity turbulence models for engineering applications. *AIAA Journal*, 32(8), 1598–1605. <http://doi.org/10.2514/3.12149>
- Mihaescu, M., Murugappan, S., Kalra, M., Khosla, S., & Gutmark, E. (2008). Large Eddy simulation and Reynolds-Averaged Navier-Stokes modeling of flow in a realistic pharyngeal airway model: An investigation of obstructive sleep apnea. *Journal of Biomechanics*, 41(10), 2279–2288. <http://doi.org/10.1016/j.jbiomech.2008.04.013>
- Mihaescu, M., Mylavarapu, G., Gutmark, E. J., & Powell, N. B. (2011). Large Eddy Simulation of the pharyngeal airflow associated with Obstructive Sleep Apnea Syndrome at pre and post-surgical treatment. *Journal of Biomechanics*, 44(12), 2221–2228. <http://doi.org/10.1016/j.jbiomech.2011.06.006>
- Min, Y. G., & Jang, Y. J. (1995). Measurements of cross-sectional area of the nasal cavity by acoustic rhinometry and CT scanning. *The Laryngoscope*, 105(7 Pt 1), 757–759. <http://doi.org/10.1288/00005537-199507000-00014>
- Moghadas, H., Abouali, O., Faramarzi, a., & Ahmadi, G. (2011). Numerical investigation of septal deviation effect on deposition of nano/microparticles in human nasal passage. *Respiratory Physiology and Neurobiology*, 177(1), 9–18. <http://doi.org/10.1016/j.resp.2011.02.011>
- Morsi, S. A., & Alexander, A. J. (2006). An investigation of particle trajectories in two-phase flow systems. *Journal of Fluid Mechanics*, 55(2), 193. <http://doi.org/10.1017/S0022112072001806>
- Mylavarapu, G., Mihaescu, M., Fuchs, L., Papatziarnos, G., & Gutmark, E. (2013). Planning human upper airway surgery using computational fluid dynamics. *Journal of Biomechanics*, 46(12), 1979–86. <http://doi.org/10.1016/j.jbiomech.2013.06.016>
- Mylavarapu, G., Murugappan, S., Mihaescu, M., Kalra, M., Khosla, S., & Gutmark, E. (2009a). Validation of computational fluid dynamics methodology used for human upper airway flow simulations. *Journal of Biomechanics*, 42(10), 1553–1559. <http://doi.org/10.1016/j.jbiomech.2009.03.035>
- Mylavarapu, G., Murugappan, S., Mihaescu, M., Kalra, M., Khosla, S., & Gutmark, E. (2009b). Validation of computational fluid dynamics methodology used for human upper airway flow simulations. *Journal of Biomechanics*, 42(10), 1553–1559. <http://doi.org/10.1016/j.jbiomech.2009.03.035>

- Reber, M., Rahm, F., & Monnier, P. (1998). The role of acoustic rhinometry in the pre- and postoperative evaluation of surgery for nasal obstruction. *Rhinology*, 36(4), 184–187. Retrieved from <http://europepmc.org/abstract/MED/9923062>
- Riazuddin, V. N., Zubair, M., Abdullah, M. Z., Ismail, R., Shuaib, I. L., Hamid, S. A., & Ahmad, K. A. (2011). Numerical study of inspiratory and expiratory flow in a human nasal cavity. *Journal of Medical and Biological Engineering*, 31(3), 201–206. <http://doi.org/10.5405/jmbe.781>
- Riazuddin, V. N., Zubair, M., Ahmadi, M., Tamagawa, M., Rashid, N. H. A., Mazlan, N., & Ahmad, K. A. (2016). Computational Fluid Dynamics Study of Airflow and Microparticle Deposition in a Constricted Pharyngeal Section Representing Obstructive Sleep Apnea Disease. *Journal of Medical Imaging and Health Informatics*, 6(6), 1507–1512. <http://doi.org/10.1166/jmihi.2016.1839>
- Riechelmann, H., O’Connell, J. M., Rheinheimer, M. C., Wolfensberger, M., & Mann, W. J. (1999). The role of acoustic rhinometry in the diagnosis of adenoidal hypertrophy in pre-school children. *European Journal of Pediatrics*, 158(1), 38–41.
- Sarkar, A., Rano, R., Mishra, K. K., & Sinha, I. N. (2005). Particle size distribution profile of some Indian fly ash—a comparative study to assess their possible uses. *Fuel Processing Technology*, 86(11), 1221–1238. <http://doi.org/10.1016/j.fuproc.2004.12.002>
- Schwab, R. J., Gefter, W. B., Hoffman, E. A., Gupta, K. B., & Pack, A. I. (1993). Dynamic Upper Airway Imaging during Awake Respiration in Normal Subjects and Patients with Sleep Disordered Breathing. *American Review of Respiratory Disease*, 148(5), 1385–1400. <http://doi.org/10.1164/ajrccm/148.5.1385>
- Segal, R. A., Kepler, G. M., & Kimbell, J. S. (2008). Effects of differences in nasal anatomy on airflow distribution: A comparison of four individuals at rest. *Annals of Biomedical Engineering*, 36(11), 1870–1882. <http://doi.org/10.1007/s10439-008-9556-2>
- Shaheen, S. M., Hooda, P. S., & Tsadilas, C. D. (2014). Opportunities and challenges in the use of coal fly ash for soil improvements – A review. *Journal of Environmental Management*, 145, 249–267. <http://doi.org/http://dx.doi.org/10.1016/j.jenvman.2014.07.005>
- Shelton, D. M., & Eiser, N. M. (1992). Evaluation of active anterior and posterior rhinomanometry in normal subjects. *Clinical Otolaryngology & Allied Sciences*, 17(2), 178–182. <http://doi.org/10.1111/j.1365-2273.1992.tb01068.x>
- Shi, H., Kleinstreuer, C., & Zhang, Z. (2007). Modeling of inertial particle transport and deposition in human nasal cavities with wall roughness. *Journal of Aerosol Science*, 38(4), 398–419. <http://doi.org/10.1016/j.jaerosci.2007.02.002>
- Sipila, J., & Suonpaa, J. (1997). A prospective study using rhinomanometry and patient clinical satisfaction to determine if objective measurements of nasal airway resistance can improve the quality of septoplasty. *European Archives of Oto-Rhino-Laryngology : Official Journal of the European Federation of Oto-Rhino-Laryngological Societies (EUFOS) : Affiliated with the German Society for Oto-Rhino-Laryngology - Head and Neck Surgery*, 254(8), 387–390.

- Sittitavornwong, S., Waite, P. D., Shih, A. M., Koomullil, R., Ito, Y., Cheng, G. C., & Wang, D. (2009). Evaluation of Obstructive Sleep Apnea Syndrome by Computational Fluid Dynamics. *Seminars in Orthodontics*, 15(2), 105–131. <http://doi.org/10.1053/j.sodo.2009.01.005>
- Subramaniam, R. P., Richardson, R. B., Morgan, K. T., Kimbell, J. S., & Guilmette, R. A. (1998). Computational Fluid Dynamics simulations of inspiratory airflow in the human nose and nasopharynx. *Inhalation Toxicology*, 10(2), 91–120. <http://doi.org/10.1080/089583798197772>
- Sung, S. J., Jeong, S. J., Yu, Y. S., Hwang, C. J., & Pae, E. K. (2006). Customized three-dimensional computational fluid dynamics simulation of the upper airway of obstructive sleep apnea. *Angle Orthodontist*, 76(5), 791–799. <http://doi.org/10.2319/071305-231>
- Suratt, P. M., Dee, P., Atkinson, R. L., Armstrong, P., & Wilhoit, S. C. (1983). Fluoroscopic and computed tomographic features of the pharyngeal airway in obstructive sleep apnea. *The American Review of Respiratory Disease*, 127(4), 487–492. <http://doi.org/10.1097/00004728-198312000-00059>
- Suzina, A. H., Hamzah, M., & Samsudin, A. R. (2003). Active anterior rhinomanometry analysis in normal adult Malays. *The Journal of Laryngology and Otology*, 117(8), 605–608. <http://doi.org/10.1258/002221503768199924>
- Tomkinson, A., & Eccles, R. (1995). Errors arising in cross-sectional area estimation by acoustic rhinometry produced by breathing during measurement. *Rhinology*, 33(3), 138–140.
- Tomkinson, A., & Eccles, R. (1998). Acoustic rhinometry: an explanation of some common artefacts associated with nasal decongestion. *Clinical Otolaryngology and Allied Sciences*, 23(1), 20–26.
- Tsuda, A., Henry, F. S., & Butler, J. P. (2013). Particle transport and deposition: basic physics of particle kinetics. *Comprehensive Physiology*, 3(4), 1437–71. <http://doi.org/10.1002/cphy.c100085>
- Versteeg, H. K., & Malalasekera, W. (1995). An Introduction to Computational Fluid Dynamics - The Finite Volume Method. *Fluid Flow Handbook*. McGraw-Hill <http://doi.org/10.2514/1.22547>
- Vos, W., De Backer, J., Devolder, a., Vanderveken, O., Verhulst, S., Salgado, R., ... De Backer, W. (2007). Correlation between severity of sleep apnea and upper airway morphology based on advanced anatomical and functional imaging. *Journal of Biomechanics*, 40(10), 2207–2213. <http://doi.org/10.1016/j.jbiomech.2006.10.024>
- Wang, S. M., Inthavong, K., Wen, J., Tu, J. Y., & Xue, C. L. (2009). Comparison of micron- and nanoparticle deposition patterns in a realistic human nasal cavity. *Respiratory Physiology and Neurobiology*, 166(3), 142–151. <http://doi.org/10.1016/j.resp.2009.02.014>
- Wang, Y., Wang, J., Liu, Y., Yu, S., Sun, X., Li, S., ... Zhao, W. (2012). Fluid–structure interaction modeling of upper airways before and after nasal surgery for obstructive sleep apnea. *International Journal for Numerical Methods in Biomedical Engineering*, 28, 528–546. <http://doi.org/10.1002/cnm>

- Wang, Z., Hopke, P. K., Ahmadi, G., Cheng, Y. S., & Baron, P. a. (2008). Fibrous particle deposition in human nasal passage: The influence of particle length, flow rate, and geometry of nasal airway. *Journal of Aerosol Science*, 39(12), 1040–1054. <http://doi.org/10.1016/j.jaerosci.2008.07.008>
- Weinhold, I., & Mlynski, G. (2004). Numerical simulation of airflow in the human nose. *European Archives of Oto-Rhino-Laryngology*, 261(8), 452–455. <http://doi.org/10.1007/s00405-003-0675-y>
- Wen, J., Inthavong, K., Tian, Z., Tu, J., Xue, C., & Li, C. (2007). Airflow patterns in both sides of a realistic human nasal cavity for laminar and turbulent conditions. *16th Australasian Fluid Mechanics Conference (AFMC)*, (December), 68–74. Retrieved from <http://espace.library.uq.edu.au/view/UQ:132285>
- Wen, J., Inthavong, K., Tu, J., & Wang, S. (2008). Numerical simulations for detailed airflow dynamics in a human nasal cavity. *Respiratory Physiology & Neurobiology*, 161(2), 125–135. <http://doi.org/10.1016/j.resp.2008.01.012>
- Wexler, D., Segal, R., & Kimbell, J. (2005). Aerodynamic effects of inferior turbinate reduction: computational fluid dynamics simulation. *Archives of Otolaryngology-Head & Neck Surgery*, 131(12), 1102–1107. <http://doi.org/10.1001/archotol.131.12.1102>
- Xi, J., & Longest, P. W. (2007). Transport and deposition of micro-aerosols in realistic and simplified models of the oral airway. *Annals of Biomedical Engineering*, 35(4), 560–581. <http://doi.org/10.1007/s10439-006-9245-y>
- Xi, J., Si, X., Kim, J. W., & Berlinski, A. (2011). Simulation of airflow and aerosol deposition in the nasal cavity of a 5-year-old child. *Journal of Aerosol Science*, 42(3), 156–173. <http://doi.org/10.1016/j.jaerosci.2010.12.004>
- Xiong, G.-X., Zhan, J.-M., Zuo, K.-J., Rong, L.-W., Li, J.-F., & Xu, G. (2011). Use of computational fluid dynamics to study the influence of the uncinate process on nasal airflow. *The Journal of Laryngology & Otology*, 125(1), 30–37. <http://doi.org/10.1017/S002221511000191X>
- Xiong, G., Zhan, J.-M., Jiang, H.-Y., Li, J.-F., Rong, L.-W., & Xu, G. (2008). Computational fluid dynamics simulation of airflow in the normal nasal cavity and paranasal sinuses. *American Journal of Rhinology*, 22(5), 477–482. <http://doi.org/10.2500/ajr.2008.22.3211>
- Xu, C., Sin, S., McDonough, J. M., Udupa, J. K., Guez, A., Arens, R., & Wootton, D. M. (2006). Computational fluid dynamics modeling of the upper airway of children with obstructive sleep apnea syndrome in steady flow. *Journal of Biomechanics*, 39(11), 2043–2054. <http://doi.org/10.1016/j.jbiomech.2005.06.021>
- Zamankhan, P., Ahmadi, G., Wang, Z., Hopke, P. K., Cheng, Y.-S., Su, W. C., & Leonard, D. (2006). Airflow and Deposition of Nano-Particles in a Human Nasal Cavity. *Aerosol Science and Technology*, 40(6), 463–476. <http://doi.org/10.1080/02786820600660903>
- Zhang, Z., & Kleinstreuer, C. (2011). Computational analysis of airflow and nanoparticle deposition in a combined nasal-oral-tracheobronchial airway model. *Journal of Aerosol Science*, 42(3), 174–194.

<http://doi.org/10.1016/j.jaerosci.2011.01.001>

- Zhang, Z., Kleinstreuer, C., Donohue, J. F., & Kim, C. S. (2005). Comparison of micro- and nano-size particle depositions in a human upper airway model. *Journal of Aerosol Science*, 36(2), 211–233. <http://doi.org/10.1016/j.jaerosci.2004.08.006>
- Zhao, K., Scherer, P. W., Hajiloo, S. a., & Dalton, P. (2004). Effect of anatomy on human nasal air flow and odorant transport patterns: Implications for olfaction. *Chemical Senses*, 29(5), 365–379. <http://doi.org/10.1093/chemse/bjh033>
- Zhao, M., Barber, T., Cistulli, P. a., Sutherland, K., & Rosengarten, G. (2013a). Simulation of upper airway occlusion without and with mandibular advancement in obstructive sleep apnea using fluid-structure interaction. *Journal of Biomechanics*, 46(15), 2586–2592. <http://doi.org/10.1016/j.jbiomech.2013.08.010>
- Zhao, M., Barber, T., Cistulli, P., Sutherland, K., & Rosengarten, G. (2013b). Computational fluid dynamics for the assessment of upper airway response to oral appliance treatment in obstructive sleep apnea. *Journal of Biomechanics*, 46(1), 142–150. <http://doi.org/10.1016/j.jbiomech.2012.10.033>
- Zhu, J. H., Lim, K. M., Thong, K. T. M., Wang, D. Y., & Lee, H. P. (2014). Assessment of airflow ventilation in human nasal cavity and maxillary sinus before and after targeted sinonasal surgery: A numerical case study. *Respiratory Physiology and Neurobiology*, 194(1), 29–36. <http://doi.org/10.1016/j.resp.2014.01.004>
- Zubair, M., Ahmad, K. A., Abdullah, M. Z., & Sufian, S. F. (2015). Characteristic airflow patterns during inspiration and expiration: experimental and numerical investigation. *Journal of Medical and Biological Engineering*, 35, 387–394.
- Zubair, M., Riazuddin, V. N., Abdullah, M. Z., Ismail, R., Shuaib, I. L., & Ahmad, K. A. (2013). Computational fluid dynamics study of the effect of posture on airflow characteristics inside the nasal cavity. *Asian Biomedicine*, 7(6), 835–840. <http://doi.org/10.5372/1905-7415.0706.247>
- Zubair, M., Riazuddin, V. N., Zulkifly, M., & Ismail, R. (2010). Airflow inside the nasal cavity: visualization using computational fluid dynamics. *Asian Biomedicine*, 4(4), 657–661.